Invited paper

K. NORDLUND✉
T.T. JÄRVI
K. MEINANDER
J. SAMELA

Cluster ion–solid interactions from meV to MeV energies

Department of Physics, University of Helsinki, P.O. Box 43, 00014 Helsinki, Finland

ABSTRACT The nature of cluster ion–surface interactions changes dramatically with the kinetic energy and mass of the incoming cluster species. In this article we review some recent work on the nature of cluster–surface interactions spanning an energy range from a few tens of meV/atom to several MeV/cluster and cluster sizes in the range of 1–300 000 atoms/cluster. We describe five possible distinct outcomes of a single cluster impact event: (i) deposition into a non-epitaxial configuration, (ii) deposition into an epitaxial configuration, (iii) crater formation by liquid flow, (iv) crater formation by hydrostatic pressure, (v) implantation.

PACS 65.80.+n; 82.60.Qr; 61.46.Hk; 02.70.Ns

1 Introduction

The interactions between energetic cluster ions and solids have become of great research interest during the last 20 years due to the development of increasingly efficient cluster ion sources [1–3] as well as finding several potential practical applications for cluster deposition. These include surface smoothing, which is already in industrial use [4], cluster burrowing for forming embedded nanoclusters [5], using clusters for hardness measurement [6] as well as achieving shallow doping of Si [7]. In spite of the wide range of examined application areas, the basic science of cluster–solid interactions is not very well understood.

Classical molecular dynamics (MD) computer simulations are well suited for studying interactions between cluster ions and solids. For elemental materials and simple compounds, these methods are efficient enough to simulate all atoms in a nanocluster, as well as millions of atoms in a solid, which is often enough to fully study the initial cluster impact event. The MD simulations (e.g., [6, 8–20]) have in conjunction with experiments (e.g., [3, 21–28]) shown that several (although often partly overlapping) regimes of physics are active during cluster impacts. The outcome can depend strongly on at least the energy and mass of the projectile, incoming angle, sample temperature and of course choice of materials.

✉ Fax: +358-9-191-50042, E-mail: kai.nordlund@helsinki.fi

The full range of possible outcomes has clearly not been fully examined, and much remains to be done and discovered in this field.

In the current article we give an overview of previously published and new MD results on the initial outcome of the cluster deposition event as a function of cluster energy and mass for single-element metallic systems. Such systems are clearly the most studied systems to date, making it possible to give a fairly comprehensive picture of possible known mechanisms and outcomes. We consider initial cluster kinetic energies ranging from a few tens of meV/atom to almost 1 MeV/atom (amounting to several tens of MeV/cluster), and a mass (cluster size) range from 1 to about 300 000 atoms.

We note that the focus on the initial outcome leaves out long-time scale effects related to thermal defect and dislocation motion, thus making the discussion most relevant to low temperatures where thermally activated effects are not so important. The long-time scale effects are difficult to study by MD methods, but can sometimes be handled with kinetic Monte Carlo methods [29]. Limiting the discussion to single-element systems leaves out intriguing effects, such as cluster burrowing [14, 23]. However, neither long-time scale nor multielemental cluster impact effects have been studied nearly enough to enable an attempt at a comprehensive picture including also these variables.

Also semiconductor and carbon-based cluster systems have been fairly extensively studied (e.g. [12, 26, 27, 30–34]), but for brevity we focus in the current paper on metals.

2 Overview of methods

The basic MD methods [35, 36] are directly well suited for examining thermal (kinetic energy < 1 eV/atom) cluster impacts on solids. If higher kinetic energies come into play, the standard MD algorithms need to be augmented by methods for handling high-energy ions and collisions between them. Fortunately these methods are well known from the field of simulation of single ion-induced cascades in solids [37–39]. To handle energetic collisions, the interatomic potentials need to be augmented with realistic high-energy repulsive potentials [40, 41]. To handle energy transfer to electrons, one needs to include an electronic stopping model [42] and possibly also a model for electron-phonon coupling [13], although considerable uncertainty remains on how strong the

latter effect is [43]. Since energetic cluster deposition effects occur far from thermodynamic equilibrium, the central parts of the simulation cell need to be handled in the microcanonical (NVE) thermodynamic ensemble, while the heat and pressure wave emanating from the impact event needs to be damped at the boundaries either with some soft scaling scheme [44] or by joining the simulation cell to an elastic medium [45]. A variable time step scheme [42] and possibly also a multiple-time step scheme [46] can be used to speed up the simulations.

The most crucial physics input to any classical MD simulation is the interatomic potential. Rather few studies have compared different potentials with respect to cluster impacts, but those which have, generally indicate that the qualitative features tend to remain the same for different potentials, while quantitative results such as sputtering yields can vary greatly [44]. In the following comparison, where we focus on qualitative description of mechanisms, we will not distinguish between potential choice as that would not affect the overall picture.

The cluster simulations are, once the algorithms are implemented in the code, typically set up as follows. The substrate is treated in a slab geometry, i.e., two directions are simulated with periodic boundary conditions while one direction is left free to model the surface. Atoms at the opposite side to the surface are fixed or damped. The substrate and cluster are first separately relaxed to allow for equilibrated thermal atomic displacements and surface relaxation. This also gives the cluster a random thermal angular momentum. The cluster is rotated by a random angle, and given a kinetic energy and deposition angle towards the surface. During impact on one hand potential energy at the interface is released to kinetic energy, on the other hand the downwards kinetic energy of the cluster is absorbed by the substrate. The system evolution is followed at least until the cluster and substrate around the impact point has cooled down to the equilibrium temperature of the substrate.

A typical low-energy deposition event is illustrated in Fig. 1.

3   Cluster deposition regimes

Even for the simple case of deposition of a single fcc metal on a single-crystalline atomically flat substrate of the same metal a surprisingly wide range of outcomes has been observed. One can distinguish between at least five different mechanisms: (i) deposition of the cluster into a non-epitaxial configuration, (ii) deposition of the cluster directly into an epitaxial configuration, (iii) crater formation by liquid flow, (iv) crater formation by hydrostatic pressure, (v) implantation. The regimes where these effects can be expected to be important as a function of cluster size and impact energy is illustrated in Fig. 2. Also reflection of the cluster back to the vacuum is a possible outcome, but we do not consider this effect here, as it does not lead to sample modification. We emphasize that the outcome is stochastic (i.e., the exact same energy and mass may lead to a different outcome) and also several mechanisms may be active in the same event. Thus the indicated boundaries are not sharp. In the following subsections the mechanisms are discussed in detail.
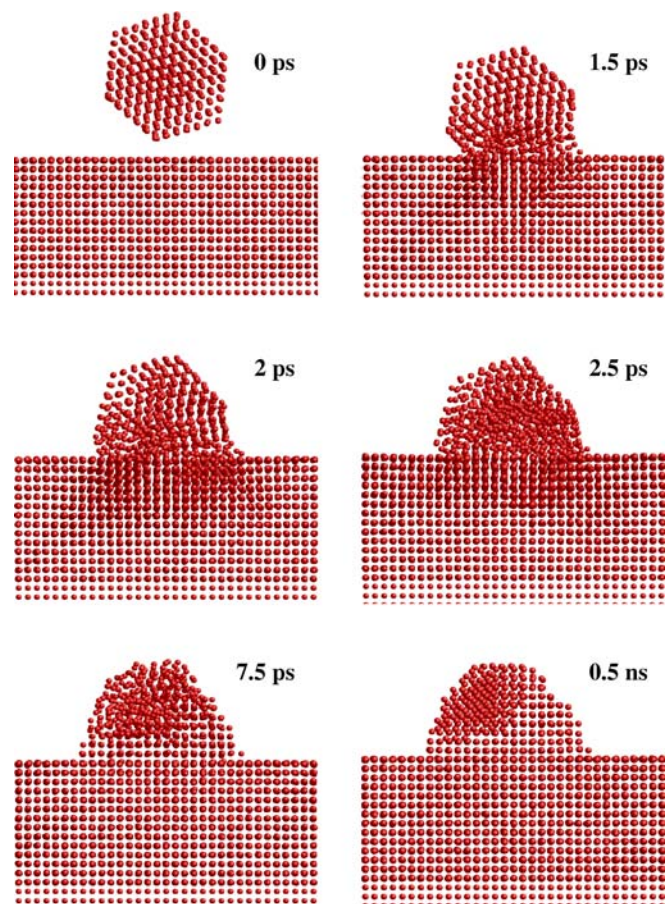

FIGURE 1   Low-energy deposition of a Cu cluster on Cu. The *snapshots* show a side view through the substrate

## 3.1   *Deposition to a non-epitaxial configuration*

When a moderate-sized or large-sized cluster impacts on a substrate at very low energies (kinetic energy/atom much less than potential energy/atom) it most likely remains in a non-epitaxial configuration, although the lowest atom planes may become epitaxial with the substrate [8, 15, 16]. This is because it is unlikely the cluster would be perfectly aligned with the substrate on impact. Such an event is illustrated in Fig. 1.

If deposition in this regime is continued, a nanocrystalline thin film will result [13, 52]. The film is most likely underdense, although even a slight increase in deposition energy can considerably increase the density of the material [52].

3.2   *Deposition to an epitaxial configuration*

If the deposited cluster is very small, or the kinetic energy is raised, the impact event may release enough energy to make the cluster partly or fully epitaxial directly on impact [15, 16, 22].

For purely thermal depositions, this behaviour can be described by a simple analytical mechanical melting model, which estimates the energy released based on geometry, surface energy and the range of the interatomic interaction [17]. The surface area in the part of the cluster closest to the substrate, and the corresponding area on the substrate surface, both release their surface potential energy to kinetic energy.
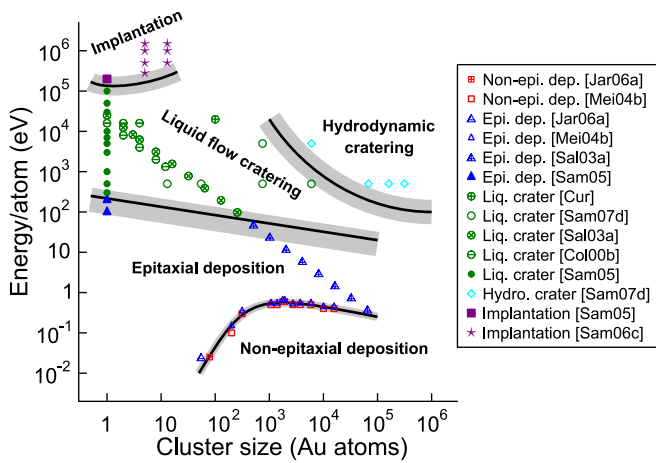
FIGURE 2 Phase diagram-like plot of the dependence of the outcome of the impact of Au clusters on Au as obtained from MD simulations. Each *symbol* is an MD data point (usually averaged over several simulations), and the *lines* are rough estimates of the expected boundaries between the different mechanisms. Note that in almost all cases the mechanisms are partly overlapping: e.g., for 200 keV Au$_1$ impacts on Au both implantation and cratering occurs (sometimes both in the same event, sometimes only one), which is emphasized by the gray shading around the lines. In such cases the data point is chosen to reflect the most dominating behaviour. The MD data are from simulations carried out between 0 and 300 K (see original references) and the time scale of a simulation is in the range 10 ps to 1 ns. All cases are from simulations with normal or near-normal impact angle. The thick grey region between the cratering and deposition regimes emphasizes that even in the deposition regime, the outcome resembles a crater down to energies of roughly 3 eV/atom. On the other hand, the boundary between epitaxial and non-epitaxial deposition can be given very accurately since this was determined deliberately in the cited papers. The references are: [Jar06a]: [17], [Mei04b]: [48], [Sal03a]: [49], [Sam05]: [44], [Cur]: current work, [Sam07d]: [50], [Col00b]: [10]. [Sam06c]: [51]. The data in [48] is for Cu, but [17] shows that the Au and Cu data are almost identical
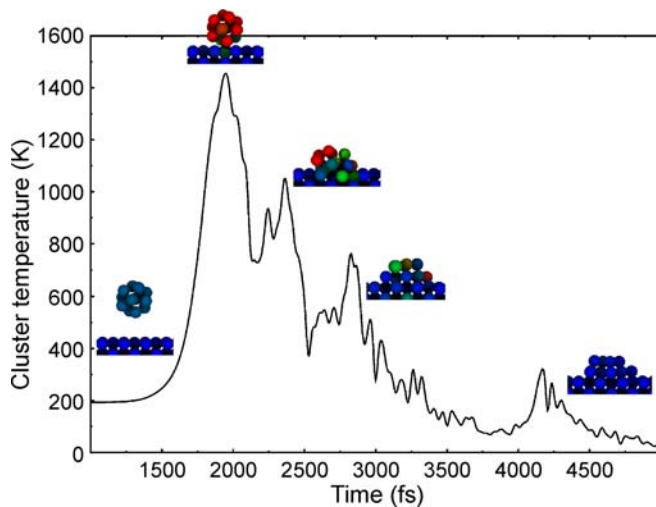
FIGURE 3 Small clusters align epitaxially if the surface energy released upon deposition is high enough to heat them above the mechanical melting point. Shown is the temperature profile of a 13 atom cluster during deposition

This leads to a strong heating of the cluster, which can melt it completely and make it epitaxial with the substrate, see Fig. 3.

Also another, less obvious, mechanism can make the cluster epitaxial rapidly after impact. The MD simulations have shown that if the cluster becomes only partly epitaxial on impact, the remaining non-epitaxial parts are often separated from the epitaxial one at the bottom by twin grain bound-
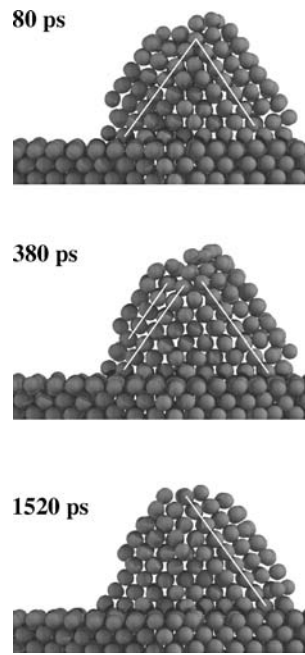
FIGURE 4 Impact of a metal nanoparticle that becomes epitaxial by dislocation reactions. The *snapshots* show a side view through the substrate. The *lines* show the location of twin grain boundaries. The twin boundary on the *left side* vanished by dislocation reactions over the ∼ 1.5 ns time scale of the simulation. For details on the mechanism, see [17]

aries [53]. These twin grain boundaries can be removed from the system by thermally activated dislocation reactions [17] (see Fig. 4).

A composite analytical model incorporating both the melting and dislocation reaction models has been shown to describe well the size limit for the cluster to become epitaxial as a function of temperature for several fcc metals and their alloys [17, 47].

When the kinetic energy/atom is in magnitude comparable to the cohesive energy/atom, the probability for it to become epitaxial increases strongly, since the downwards kinetic energy is transformed into heat which can melt the cluster [52].

As a new result, we now describe that the mechanical melting model introduced above and in [17] can be generalized to account for the effect of non-negligible deposition energy. The original formulation equated the rise in temperature needed to melt a landing cluster with the surface energy released from the disappearing surface area,

$$\frac{3}{2} N k_{\mathrm{B}} \Delta T = \frac{\Delta E}{2} , \qquad (1)$$

where $\Delta T = T_{\mathrm{melt}} - T_{\mathrm{i}}$, T_{i} being the cluster's initial temperature and ΔE the surface energy released.

In the case of energetic particle deposition, a part of the deposition energy can simply be added to the energy contributing to the transient heating. The right hand side of the above equation is thus modified to $\Delta E + c E_{\mathrm{k}}$, where c is the fraction of the deposition energy E_{k} that is converted to heat in the particle. The remaining fraction goes to heating the substrate and to the shock waves generated by the impact. In the present discussion, we simply assume that half of the energy goes to heating, that is, $c = 0.5$.
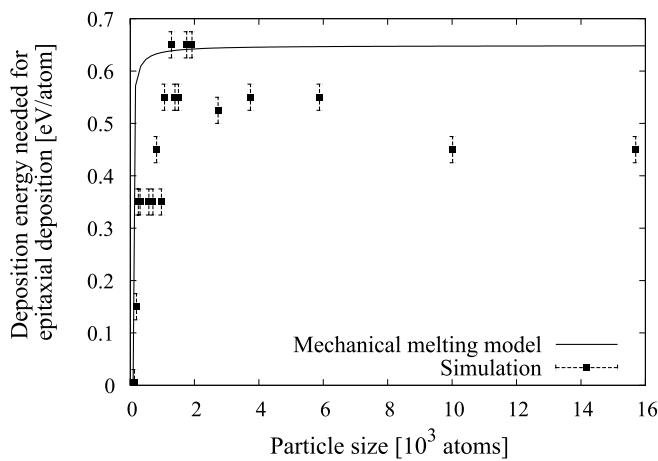
FIGURE 5 The energy required for epitaxial deposition as a function of particle size. The simulations are from [48]

The energy required to epitaxially deposit a particle of N atoms thus becomes

$$\frac{E_k}{N} = \frac{1}{c}\left[3k(T_{melt} - T_i) - \frac{\Delta E}{N}\right]. \tag{2}$$

Figure 5 shows the prediction of this model for copper compared to simulation results from [48]. The energy required for epitaxial deposition quickly rises, saturating for particles larger than ~ 2000 atoms. While the model shows perfect saturation, simulation results indicate a slight decrease in the required energy. This is mainly because the model ignores effects related to heat conduction. For the larger particles, it takes time to dissipate heat to the substrate, leaving the particle at a high temperature for a longer time.

3.3 *Cratering by liquid flow*

When the energy/atom is raised high enough that the cluster atoms can penetrate the surface, implantation of the atoms of course results. However, in dense metals and for heavy atom projectiles, a heat spike almost always results from a cascade. Thus if the implantation depth is close to the surface, the heat spike most likely ruptures the surface and the ensuing microexplosion, liquid flow and coherent displacement phenomena lead to a cascade outcome completely dominated by the surface [54–56]. For single ions, this effect is now quite well understood due to a range of simulation and experimental studies which are in good agreement with each other [54, 57–64]. Small clusters of comparable energy show very similar cratering behaviour [10, 65, 66] as the single ions; since the heat spikes tend to be enhanced due to cascade overlap, the cratering probability and crater sizes are even larger than for single ions. This is reflected in very high sputtering yields due to the emission of large clusters from the crater rims [24, 51].

A typical massive heat spike event leading to cratering and cluster emission is shown in Fig. 6. A curious side effect in these kinds of events is that since the ejected clusters are very hot, they emit atoms and clusters by evaporation (i.e., they boil). About half of these emitted atoms are ejected back towards the surface, making the final sputtering yield considerably smaller than the initial one. A systematic study of this
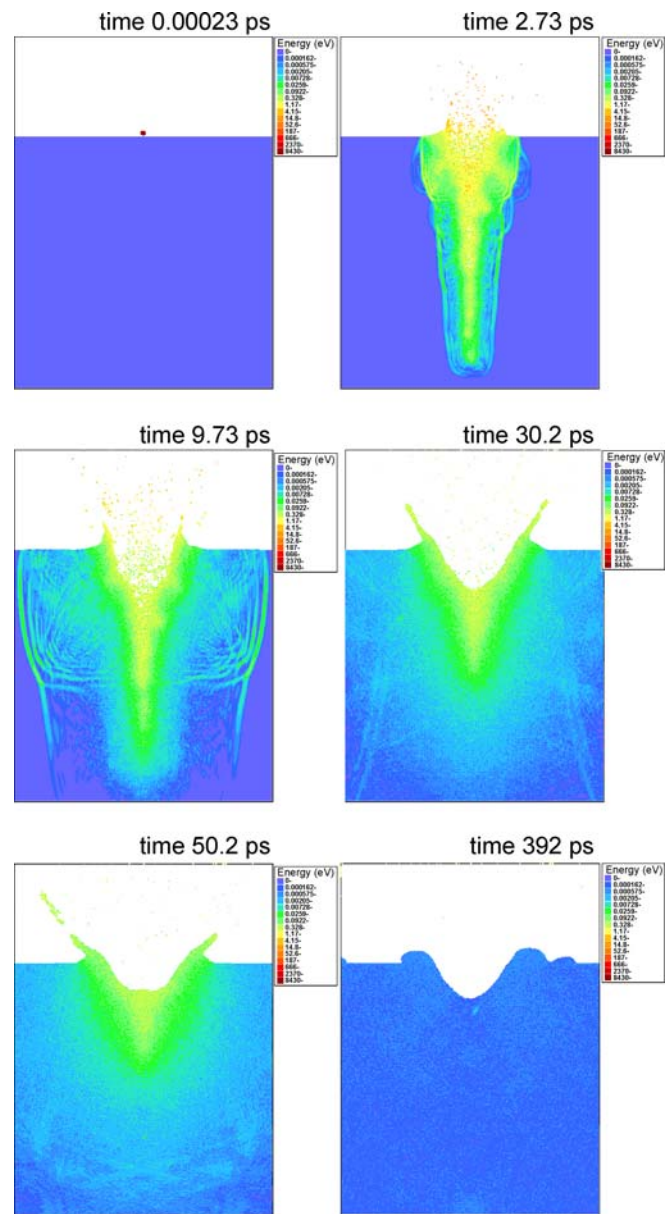
FIGURE 6 Cratering by a 20 keV/atom Au$_{100}$ atom cluster impact in Au. The *snapshots* show a 2 unit cell thick slice through the center of the simulation cell. The atoms are shown as *small squares*; since the number of atoms in this slice is about 600 000 (the whole simulation cell had about 100 million atoms), the interior of the cell looks like a continuum even though the simulation is fully atomistic. Note the pressure waves emanating from the cascade and the massive sputtering. The *colors* indicate the kinetic energy of the atoms on a logarithmic scale

effect for 20 keV Xe impacts on Au showed that about 90% of the clusters break up, and this can reduce the final sputtering yield by 30% compared to the initial one [67].

3.4 *Cratering by hydrodynamics*

In large cluster cratering events such as those illustrated in Fig. 6, the behaviour of the system clearly starts to visually resemble that expected in macroscopic systems, such as dropping of a metal pellet on water. Indeed the formation of a corona and fingers which break up due to

the Rayleigh instability [68] is well known in hydrodynamics [69]. A natural question thus arises: If the cluster size is continuously increased at the same energy/atom, when does the behaviour make a full transition to macroscopic continuum-like behaviour?

We have very recently addressed this question for crater formation [50]. While the single ion-induced craters form by liquid flow (see above), the macroscopic ones such as those observed on moons and planets form due to the formation of a transient high-pressure region inside the material [69]. It is clear that if the velocity is kept constant and corresponding to that used in the macroscopic regime, the atomic behaviour must at some point transit to the macroscopic-like one. To examine this, we bombarded Au substrates with Au clusters in sizes ranging from 13 to 300 000 atoms at a velocity of about 20 000 km/s (500 eV/atom), corresponding to typical meteorite impact velocities. We analyzed the local density of atoms below the projectile to find whether a high-pressure region is formed.

The results showed that for an Au projectile size of about 50 000 atoms, the behaviour indeed changes to the macroscopic-like one, with the formation of a high-pressure core which leads to crater formation without liquid flow. The transition region is roughly indicated in Fig. 2, but due to the scarcity of data we emphasize that the transition point is reliably given only along the energy value of 500 eV/atom.

3.5   *Implantation*

Although cratering events also can involve penetration of the projectile atoms through the surface, in the cratering regime the surface effects strongly dominate the outcome. Hence only when the cluster energy is high enough that the cluster atoms penetrate deep into substrate with no noticeable surface effects, can one consider the outcome akin to conventional ion implantation. Simulations [44] and experiments [24] of Au irradiation indicate this occurs in gold around energies of the order of 100 keV/atom. For lighter targets with higher melting points the limit can be considerably lower since heat spikes are smaller.

In the implantation regime, one can as a first approximation consider that the ions penetrate the sample as independent single ions. However, at least two cluster-related effects can occur. The first is the so-called "clearing-the-way" effect [70, 71], in which the front ions in a cluster clear the way for the following ones, leading to a reduced average nuclear stopping. The magnitude of this effect has been somewhat controversial, as some experiments have reported it not being observed at all [26]. MD simulations of the same conditions indicated that the effect is present, but so small it is not observable in the experiments [72]. A curious side effect of the clearing-the-way effect is that it can, due to correlated motion of the cluster atoms, also lead to some cluster atoms gaining kinetic energy in many-body interactions [51].

Another cluster-related effect in the implantation regime is the enhancement of heat spikes. Since the cluster ions penetrate the same region of the sample at the same time, it is highly likely that the heat spikes they produce overlap. Thus leads to a strongly enhanced redistribution (mixing) of atoms [72], an effect which has been experimentally observed
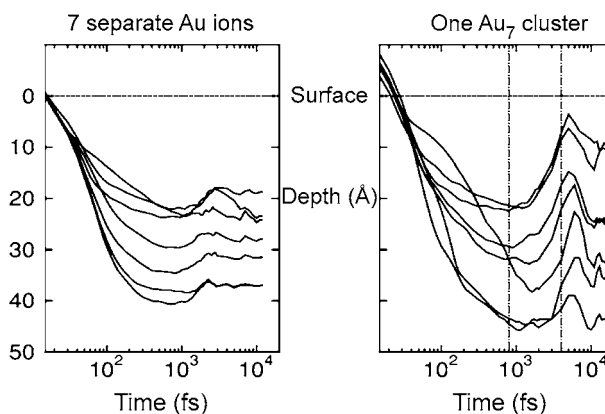
FIGURE 7   Development of the *z* coordinate of 7 Au ions implanted at 5 keV/atom into Cu either separately from each other (*left*), or in an Au$_7$ cluster (*right*). Each *line* shows the penetration depth of the 7 Au atoms as a function of time. In the cluster case, visual inspection showed that massive heat spikes developed, which lead to a redistribution of atoms. This is reflected in the time dependence of the positions of the Au atoms: In the cluster, but not the single ion, case they are strongly changed after 1 ps in the heat spike phase. Data from [72]

as an increased straggling of the ion range distribution [26]. The effect is illustrated in Fig. 7.

4   Discussion and conclusions

A natural question relating to all the previously described MD simulation results is whether they are really relevant to experiments, where the time scales are much longer than those accessible to MD. It is well known that single adatoms migrate already at room temperature in several metals [73], raising the question whether the surface features formed either by cratering or deposition are stable at all. However, larger atom agglomerates are more stable than single adatoms [29], and for instance the experiments by Donnelly and Birtcher have clearly shown that Au craters are stable up to temperatures of $\sim$ 600 K [64]. Thus it is reasonable to assume that at least the larger surface structures formed in simulations are stable at room temperature. Small deposited clusters can be expected to flatten out to monolayer islands [29].

A more serious issue regarding correspondence to experiments is whether the MD simulations of clusters impacting on single-crystalline substrates is relevant at all to experimental situations where most metal surfaces are oxidized. Clearly direct reproduction of the MD simulation conditions would require ultra-high vacuum conditions and in situ sample cleaning for all other metals except Au. A natural continuation of the MD simulations could be to address the issue of the effects of surface oxidation on the cluster impact outcome, which would also help in identifying economically viable application areas. In fact very recent studies have examined the effects of a surface oxide on silicon on the outcome of cluster deposition events [34].

In conclusion, we have described five distinct, although sometimes simultaneously occurring, regimes of cluster ion impact mechanisms: (i) deposition of the cluster into a non-epitaxial configuration, (ii) deposition of the cluster directly into an epitaxial configuration, (iii) crater formation by liquid flow, (iv) crater formation by hydrostatic pressure, (v) implan-

tation. We also roughly indicated in which cluster mass and energy ranges these can be expected to occur for the case of Au impacts on Au.

REFERENCES

1 H. Hahn, R.S. Averback, J. Appl. Phys. **67**, 1113 (1990)
2 R.L. McEahern, W.L. Brown, M.F. Jarrold, M. Sosnovski, G. Takaoka, H. Usui, I. Yamada, J. Vac. Sci. Technol. A **9**, 3105 (1991)
3 H. Haberland, M. Moseler, Y. Qiang, O. Rattunde, T. Reiners, Y. Thurner, Surf. Rev. Lett. **3**, 887 (1996)
4 R. MacCrimmon, J. Hautala, M. Gwinn, S. Sherman, Nucl. Instrum. Methods Phys. Res. B **242**, 427 (2005)
5 C. Zimmermann, M. Yeadon, M. Ghaly, K. Nordlund, J.M. Gibson, R.S. Averback, U. Herr, K. Samwer, Phys. Rev. Lett. **83**, 1163 (1999)
6 Z. Insepov, R. Manory, J. Matsuo, I. Yamada, Phys. Rev. B **61**, 8744 (2000)
7 K. Goto, M. Kase, J. Matsuo, I. Yamada, D. Takeuchi, N. Toyoda, N. Shimada, Boron Doping by Decaborane (2000)
8 M. Ghaly, R.S. Averback, In: *Beam Solid Interactions: Fundamentals and Applications Symposium*, ed. by M. Nastasi, L.R. Harriott, N. Herbots, R.S. Averback (MRS, ADDRESS, 1993), vol. 279, pp. 17–22
9 R. Aderjan, H.M. Urbassek, Nucl. Instrum. Methods Phys. Res. B **164**/**165**, 697 (2000)
10 T.J. Colla, H.M. Urbassek, Nucl. Instr. Meth. Phys. Res. B **164**/**165**, 687 (2000)
11 H. Haberland, Z. Insepov, M. Moseler, Phys. Rev. B **51**, 11 061 (1995)
12 L.P. Allen, Z. Insepov, C.S.D.B. Fenner, W. Brooks, K.S. Jones, I. Yamada, J. Appl. Phys. **92**, 3671 (2002)
13 Q. Hou, M. Hou, L. Bardotti, B. Prével, P. Mélinon, A. Perez, Phys. Rev. B **62**, 2825 (2000)
14 J. Frantz, K. Nordlund, Phys. Rev. B **67**, 075 415 (2003)
15 K. Meinander, J. Frantz, K. Nordlund, J. Keinonen, Thin Solid Films **425**, 297 (2002)
16 K. Meinander, T.T. Järvi, K. Nordlund, Appl. Phys. Lett. **89**, 253 109 (2006)
17 T. T. Järvi, A. Kuronen, K. Meinander, K. Albe, K. Nordlund, Phys. Rev. B **75**, 115 422 (2007)
18 A. Awasthi, S.C. Hendy, P. Zoontjens, S.A. Brown, Phys. Rev. Lett. **97**, 186 103 (2006)
19 A. Awasthi, S.C. Hendy, P. Zoontjens, S.A. Brown, F. Natali, Phys. Rev. B **76**, 115 437 (2007)
20 R. Reichel, J.G. Partridge, F. Natali, T. Matthewson, S.A. Brown, A. Lassesson, D.M.A. Mackensie, A. Ayesh, K.C. Tee, A. Awasthi, S.C. Hendy, Appl. Phys. Lett. **89**, 213 105 (2006)
21 H.H. Andersen, H.L. Bay, J. Appl. Phys. **45**, 953 (1974)
22 M. Yeadon, J.C. Yang, M. Ghaly, K. Nordlund, R.S. Averback, J.M. Gibson, J. Electron. Microsc. Suppl. S **48**, 1075 (1999)
23 C. Zimmermann, M. Yeadon, K. Nordlund, J.M. Gibson, R.S. Averback, U. Herr, K. Samwer, Phys. Rev. B **64**, 085 419 (2001)
24 S. Bouneau, A. Brunelle, S. Della-Negra, J. Depauw, D. Jacquet, Y.L. Beyec, M. Pautrat, M. Fallavier, J.C. Poizat, H.H. Andersen, Phys. Rev. B **65**, 144 106 (2002)
25 S.P.R.E. Palmer, H.-G. Boyen, Nat. Mater. **2**, 443 (2003)
26 H.H. Andersen, A. Johansen, M. Olsen, V. Touboltsev, Nucl. Instrum. Methods Phys. Res. B **212**, 56 (2003)
27 R. Webb, A. Chatzipanagiotou, Nucl. Instrum. Methods Phys. Res. B **242**, 413 (2006)
28 R. Espiau de Lamaestre, H. Bernas, Phys. Rev. B **73**, 125 317 (2006)
29 J. Frantz, M. Rusanen, K. Nordlund, I.T. Koponen, J. Phys.: Condens. Matter **16**, 2995 (2004)
30 R. Webb, M. Kerford, E. Ali, M. Dunn, L. Knowles, K. Lee, J. Mistry, F. Whitefoot, Surf. Interf. Anal. **31**, 297 (2001)

31 J. Tarus, K. Nordlund, Nucl. Instrum. Methods Phys. Res. B **212**, 281 (2003)
32 V. Popok, S. Prasalovich, E. Campbell, Surf. Sci. **566**/**568**, 1179 (2004)
33 A. Harjunmaa, J. Tarus, K. Nordlund, J. Keinonen, Eur. Phys. J. D **43**, 165 (2007)
34 J. Samela, K. Nordlund, V.N. Popok, E.E.B. Campbell, Phys. Rev. B **77**, 075 309 (2008)
35 M.P. Allen, D.J. Tildesley, *Computer Simulation of Liquids* (Oxford University Press, Oxford, England, 1989)
36 A.R. Leach, *Molecular modelling: principles and applications*, 2nd edn. (Pearson Education, Harlow, England, 2001)
37 T. Diaz de la Rubia, R.S. Averback, R. Benedek, W.E. King, Phys. Rev. Lett. **59**, 1930 (1987), see also erratum: Phys. Rev. Lett. **60**, 76 (1988)
38 H.M. Urbassek, K.T. Waldeer, Phys. Rev. Lett. **67**, 105 (1991)
39 K. Nordlund, M. Ghaly, R.S. Averback, M. Caturla, T. Diaz de la Rubia, J. Tarus, Phys. Rev. B **57**, 7556 (1998)
40 J.F. Ziegler, J.P. Biersack, U. Littmark, *The Stopping and Range of Ions in Matter* (Pergamon, New York, 1985)
41 K. Nordlund, N. Runeberg, D. Sundholm, Nucl. Instrum. Methods Phys. Res. B **132**, 45 (1997)
42 K. Nordlund, Comput. Mater. Sci. **3**, 448 (1995)
43 K. Nordlund, L. Wei, Y. Zhong, R.S. Averback, Phys. Rev. B (Rapid Commun.) **57**, 13 965 (1998)
44 J. Samela, J. Kotakoski, K. Nordlund, J. Keinonen, Nucl. Instrum. Methods Phys. Res. B **239**, 331 (2005)
45 M. Moseler, J. Nordiek, H. Haberland, Phys. Rev. B **56**, 15 439 (1997)
46 M. Tuckerman, B.J. Berne, G.J. Martyna, J. Chem. Phys. **97**, 1990 (1992)
47 T.T. Järvi, A. Kuronen, K. Nordlund, K. Albe (2008), to be published
48 K. Meinander, K. Nordlund, J. Keinonen, Nucl. Instrum. Methods Phys. Res. B **242**, 161 (2006)
49 E. Salonen, K. Nordlund, J. Keinonen, Nucl. Instrum. Methods Phys. Res. B **212**, 286 (2003)
50 J. Samela, K. Nordlund, (2008), submitted for publication
51 J. Samela, K. Nordlund, Phys. Rev. B **76**, 125 434 (2007)
52 K. Meinander, T. Clauß, K. Nordlund, In: *Growth, Modification, and Analysis by Ion Beams at the Nanoscale*, vol. 908E of MRS Symposium Proceedings, ed. by W. Jiang (MRS, Warrendale, PA, USA, 2006), pp. 0908–OO14–20.1.
53 J.P. Hirth, J. Lothe, *Theory of Dislocations*, 2nd edn. (Krieger, Malabar, Florida, 1992)
54 M. Ghaly, R.S. Averback, Phys. Rev. Lett. **72**, 364 (1994)
55 K. Nordlund, J. Keinonen, M. Ghaly, R.S. Averback, Nature **398**, 49 (1999)
56 K. Nordlund, J. Keinonen, M. Ghaly, R.S. Averback, Nucl. Instrum. Methods Phys. Res. B **148**, 74 (1999)
57 W. Jäger, K.L. Merkle, Philos. Mag. A **57**, 479 (1988)
58 R.C. Birtcher, S.E. Donnelly, Phys. Rev. Lett. **77**, 4374 (1996)
59 S.E. Donnelly, R.C. Birtcher, Phys. Rev. B **56**, 13 599 (1997)
60 M. Ghaly, K. Nordlund, R.S. Averback, Philos. Mag. A **79**, 795 (1999)
61 M. Morgenstern, T. Michely, G. Comsa, Philos. Mag. A **79**, 7756 (1999)
62 E. Bringa, K. Nordlund, J. Keinonen, Phys. Rev. B **64**, 235 426 (2001)
63 K. Nordlund, J. Tarus, J. Keinonen, S.E. Donnelly, R.C. Birtcher, Nucl. Instrum. Methods Phys. Res. B **206**, 189 (2003)
64 S.E. Donnelly, R.C. Birtcher, K. Nordlund, In: *Engineering Thin Films and Nanostructures with Ion Beams*, ed. by E.J. Knystautas (Marcel Dekker, New York, 2005), Chap. Single Ion Induced Spike Effects on Thin Metal Films: Observation and Simulation, pp. 7–78
65 K. Nordlund, K.O.E. Henriksson, J. Keinonen, Appl. Phys. Lett. **79**, 3624 (2001)
66 K.O.E. Henriksson, K. Nordlund, J. Keinonen, Phys. Rev. B **76**, 245 428 (2007)
67 K.O.E. Henriksson, K. Nordlund, J. Keinonen, Phys. Rev. B **71**, 014 117 (2005)
68 L. Rayleigh, Proc. R. Soc. London **29**, 71 (1879)
69 R.M. Schmidt, K.R. Housen, Int. J. Impact Eng. **5**, 543 (1987)
70 P. Sigmund, J. Phys. Colloque C2 **50**, 175 (1989)
71 V.I. Shulga, P. Sigmund, Nucl. Instrum. Methods Phys. Res. B **47**, 236 (1990)
72 J. Peltola, K. Nordlund, Phys. Rev. B **68**, 035 419 (2003)
73 H. Brune, Surf. Sci. Rep. **31**, 121 (1998)